

# A complete description of thermodynamic stabilities of molecular crystals

Venkat Kapil\*

*Yusuf Hamied Department of Chemistry, University of Cambridge,  
Lensfield Road, Cambridge, CB2 1EW, UK and  
Laboratory of Computational Science and Modeling, Institut des Matériaux,  
École Polytechnique Fédérale de Lausanne, 1015 Lausanne, Switzerland*

Edgar A Engel†

*TCM Group, Cavendish Laboratory, University of Cambridge,  
J. J. Thomson Avenue, Cambridge CB3 0HE, United Kingdom*

(Dated: June 7, 2022)

Accurate prediction of the stability of molecular crystals is a longstanding challenge, as often minuscule free energy differences between polymorphs are sensitively affected by the description of electronic structure, the statistical mechanics of the nuclei and the cell, and thermal expansion. The importance of these effects has been individually established, but rigorous free energy calculations, which simultaneously account for all terms, have been prevented by prohibitive computational costs. Here we reproduce the experimental stabilities of polymorphs of three prototypical compounds – benzene, glycine, and succinic acid – by computing rigorous *ab initio* Gibbs free energies, at a fraction of the cost of conventional harmonic approximations. This is achieved by a bottom-up approach, which involves generating machine-learning potentials to calculate surrogate free energies and subsequently calculating true *ab initio* free energies using inexpensive free energy perturbations. Accounting for all relevant physical effects is no longer a daunting task and provides the foundation for reliable structure predictions for more complex systems of industrial importance.

Keywords: polymorphism, free energy, machine learning

Molecular crystals are ubiquitous in the pharmaceutical industry [1] and show great promise for applications in organic photovoltaics [2], gas absorption [3], and the food [4], pesticide [5] and fertilizer industries [6]. Their tendency to exhibit polymorphism i.e. to exist in multiple crystal structures, on one hand provides a mechanism to tune properties by controlling crystal structure [7], and on the other hand introduces the challenge of synthesising and stabilizing crystal structures with desired properties [8]. While thermodynamic stability at the temperature and pressure of interest is sufficient (although not necessary<sup>1</sup>) to ensure long-term stability, simply understanding thermodynamic stability already poses a formidable challenge. This is particularly true for pharmaceuticals, where free energy differences between drug polymorphs are often smaller than 1 kJ/mol [9], leading to the risk of the drug transforming into a less soluble and consequently less effective form during the course of manufacturing, storage or shelf-life [10, 11]. Indeed, the problem of late appearing drug polymorphs is widespread [12, 13].

The pharmaceutical industry therefore spends con-

siderable resources on high-throughput crystallization experiments to screen for (meta-)stable, synthesizable polymorphs [14], into which the target polymorph may decay. However, crystallization experiments do not probe thermodynamic stability, and conclusive studies of the impact of temperature changes after crystallisation on the stability of polymorphs (i.e. their monotropic or enantiotropic nature [15]) are often prevented by limited sample quantities. Hence the appeal of theoretical crystal structure prediction (CSP) [16] based on the thermodynamic stability of polymorphs, which promises to guide industrial drug design and to complement crystallization experiments [17].

Despite the demonstrable value of CSP for many classes of materials [21–32], and the continuing progress evidenced by a series of blind tests [33–38], the success of CSP for molecular crystals has been limited by the inability to routinely predict the relative stability of competing candidate structures [38]. This is largely because the methods used for stability rankings typically ignore or approximate the subtle interplay of several effects, such as intricate inter-molecular interactions [39], the (quantum) statistical mechanics of the nuclei [40] and the unit cell [41], and thermal expansion [42], thereby incurring errors larger than the free energy differences of interest. Indeed, the importance of these effects has been demonstrated, albeit in isolation. For instance, harmonic [43–46] and anharmonic [40, 41] vibrational free energies have been

\* Correspondence email address: vk380@cam.ac.uk

† Correspondence email address: eae32@cam.ac.uk

<sup>1</sup> kinetics may protect thermodynamically metastable structures from decaying almost indefinitely

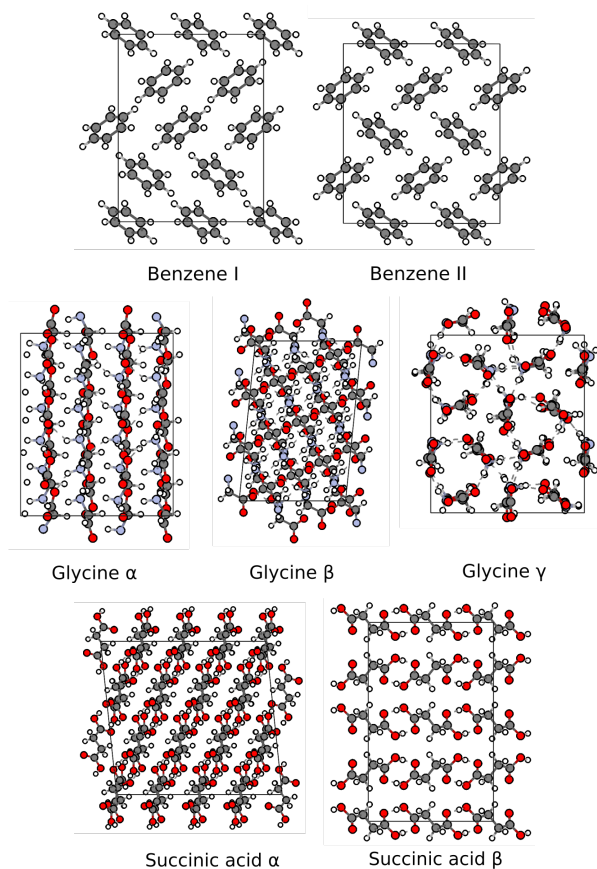


Figure 1. Structures of forms I and II of benzene containing 16 molecules, forms  $\alpha$ ,  $\beta$ , and  $\gamma$  of glycine containing 24 molecules, and forms  $\alpha$  and  $\beta$  of succinic acid containing 24 molecules. Hydrogen, carbon, nitrogen, and oxygen atoms are shown in white, gray, blue, and red, respectively.

studied on the basis of force-fields or semi-local DFT, thereby ignoring their interplay with other important effects like Pauli repulsion, many-body dispersion, and fluctuations of the simulation cell. While all of these effects can be simultaneously and accurately be accounted for using *ab initio* path integral (PI) free energy calculations [47], the cost of such simulations has generally necessitated the use of less accurate but computationally cheaper approximate methods [48].

This work addresses the problem of accurately ranking a *preexisting* set of polymorphs of complex molecular crystals by thermodynamic stability. Following in the footsteps of Ref. [49], we calculate accurate *ab initio* Gibbs free energies of diverse, complex molecular crystals while leveraging accurate machine-learning potentials [50] (MLPs) to mitigate computational costs. We demonstrate that computing MLP free energies while exactly accounting for the statistical mechanics of the nuclei and the cell, and subsequently promoting them to

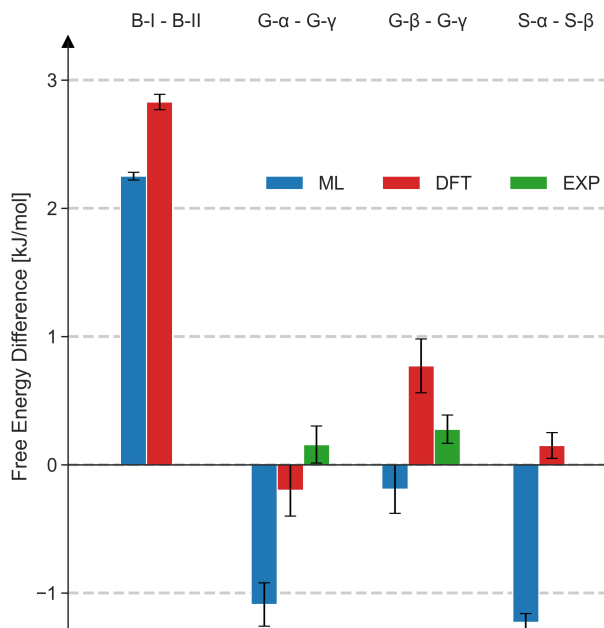


Figure 2. Path integral (PI) Gibbs free energy differences between forms I and II of benzene (B-I and B-II),  $\alpha$ ,  $\beta$ , and  $\gamma$ -glycine (G- $\alpha$ , G- $\beta$  and G- $\gamma$ ), and  $\alpha$  and  $\beta$ -succinic acid (S- $\alpha$  and S- $\beta$ ) calculated using PBE0-MBD based machine-learning potentials (MLPs) (blue) and corrected to the *ab initio* PBE0-MBD DFT level using free energy perturbation (red). Experimental data [18–20] are shown in green.

*ab initio* hybrid-functional DFT free energies using free energy perturbation (FEP), leads to consistently correct stability predictions for polymorphs of three prototypical molecular crystals – benzene, glycine, and succinic acid – and thus constitutes an avenue to predictive CSP for complex molecular crystals of industrial importance. While we focus on ambient pressure and temperatures of 100 K and 300 K, respectively, we also compute gradients of Gibbs free energies as indicators for the monotropic or enantiotropic nature of the polymorphs, and note that our free energy calculations naturally generalize to the calculation of full  $p - T$  phase diagrams.

## RESULTS

In order to predict rigorous relative stabilities, we combine PI thermodynamic integration [40, 48] in the constant pressure ensemble (thereby accounting for anharmonic quantum nuclear motion and the fluctuations and thermal expansion of the cell) with DFT calculations with the hybrid PBE0 functional and the many-body dispersion correction of Tkatchenko *et al.* (in the following referred to as PBE0-MBD). PBE0-MBD

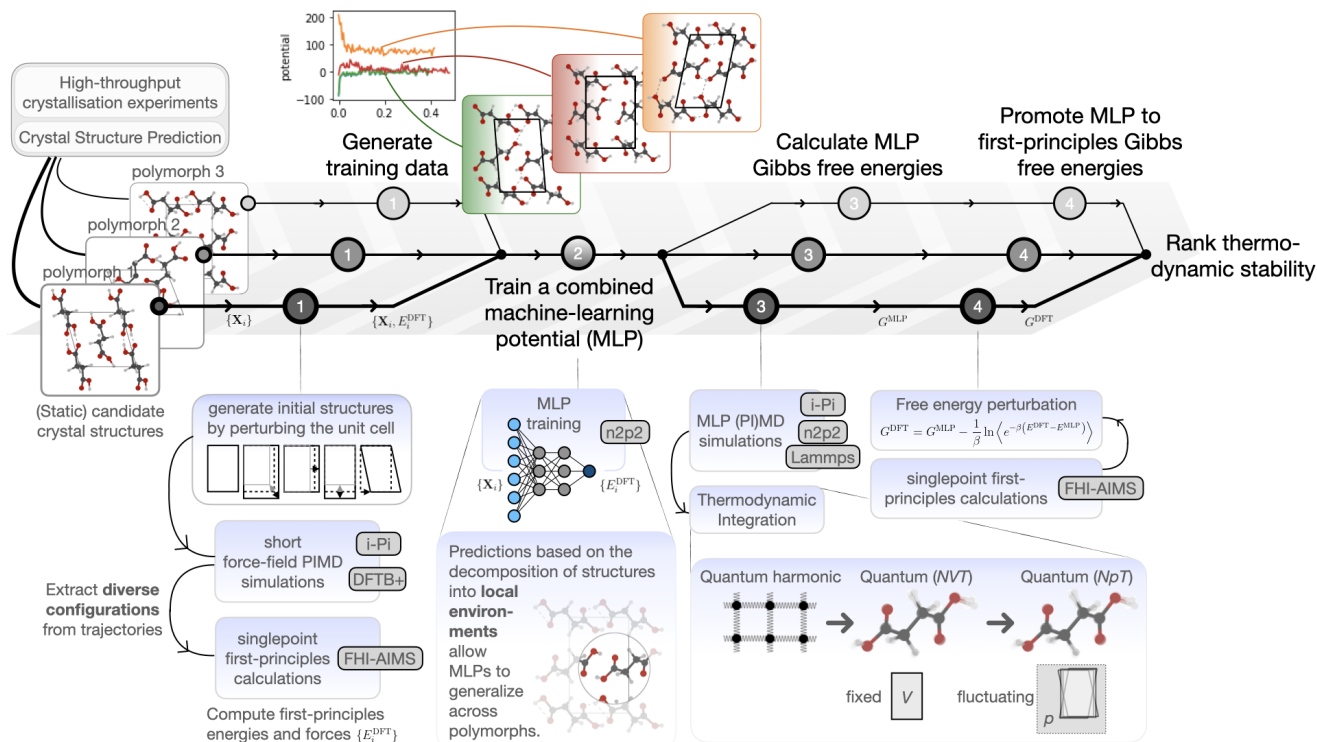


Figure 3. Schematic representation of the workflow for computing *ab initio*, quantum anharmonic Gibbs free energies for candidate crystal structures. The upper half of the figure shows the main steps: (1) generating *ab initio* reference data on which to (2) train a combined MLP, which can then be used to (3) compute MLP Gibbs free energies, which one can finally (4) promote to *ab initio* Gibbs free energies. The lower half (shaded in blue) details the key aspects of how each of these steps is performed in practice.

provides an accurate description of inter-molecular interactions, as benchmarked using experimental and CCSD(T) lattice energies for various molecular crystals, including form I of benzene and  $\alpha$ -glycine [51, 52].

Since direct calculation of Gibbs free energies from *ab initio* PI thermodynamic integration is prevented by the cost of the required energy and force evaluations [48], *ab initio* Gibbs free energies are calculated in a four-step process, as depicted schematically in Fig. 3. The first and second step involve the generation of PBE0-MBD reference data and the construction of MLPs thereupon. Both are detailed in the methods section, use readily available and well-documented software, and can easily be repeated for almost any compound of interest at the cost of a few thousand PBE0-MBD unit-cell reference calculations. Crucially, accurate MLPs, which predict energies and forces of extended structures on the basis of local contributions, do not necessarily require reference data for the extended structures, provided all relevant local environments are included [53]. In cases which do not benefit from the small unit cell sizes considered in this work, reference data for smaller “disordered” structures

should thus provide an alternative to explicit *ab initio* calculations for large crystal structures. In a third step, Gibbs free energies for the much larger simulation supercells are calculated using PI thermodynamic integrations based on the surrogate MLPs, which are many orders of magnitude cheaper to evaluate than the *ab initio* reference method. However, residual errors with respect to the *ab initio* free energies arise from the imperfect reproduction of the *ab initio* potential energy surface by the MLPs [49, 54, 55]. The typical errors in MLP predictions of configurational energies are shown in Table I. These may arise from the lack of long-range interactions in the parametrization of the MLP [56], the incomplete description of local atomic environments [57], or simply due to insufficient training data or the stochastic nature of the training procedure. In a fourth and final step we eliminate the associated errors to obtain true *ab initio* Gibbs free energies by computing the difference between the MLP and PBE0-MBD free energies using FEP [49].

We demonstrate the effectiveness of the scheme on a diverse set of prototypical systems: benzene is the archetypal rigid, van-der-Waal’s bonded molecular

System	reference data	energy RMSE [kJ/mol]
Benzene	1,000	1.2
Glycine	4,000	1.6
Succinic acid	2,000	2.3

Table I. Number of single-point PBE0-MBD calculations underlying each MLP, and their respective root-mean-square errors (RMSE) in predicting energies on a separate test set of configurations from PI simulations of the experimental unit cells.

crystal, while glycine prototypes flexible zwitter-ionic systems, and succinic acid represents general hydrogen-bonded systems. We focus on free energy differences at ambient pressure and 100 K for benzene and succinic acid and 300 K for glycine, but full  $p$ - $T$  phase-diagrams can be calculated analogously. For each compound we consider the stable polymorph and its closest competitors: forms I and II of benzene [58],  $\alpha$ ,  $\beta$ , and  $\gamma$ -glycine [59], and  $\alpha$  and  $\beta$ -succinic acid [60]. The nearly orthorhombic simulation supercells shown in Fig. 1, which contain equivalent numbers of molecules for all polymorphs of the same compound, ensure uniform sampling of the vibrational Brillouin zone (BZ), and that the centre-of-mass free energy term largely cancels out in free energy differences between polymorphs.

As shown in Fig. 2, the final *ab initio* Gibbs free energies (shown in black) reproduce the greater stability of form I over form II of benzene [61], of  $\alpha$  over  $\beta$ -succinic acid [62], the metastability of  $\beta$ -glycine [20], and the near degeneracy of  $\alpha$  and  $\gamma$ -glycine [19]. Moreover, our Gibbs free energy differences are in good agreement with calorimetry data for glycine to within statistical and experimental uncertainties. Meanwhile, the MLP-based stability predictions (shown in red) are only limited by the accuracy with which the MLPs reproduce the *ab initio* potential energy surface (see Table I) and, consequently, correctly reproduce the greater stability of form I of benzene compared to form II. At the same time, the incorrect MLP-based stability predictions for succinic acid and glycine highlight the critical importance of the final FEP step. Glycine and succinic acid are zwitter-ionic and have delocalized ions, respectively, necessitating the explicit treatment of long-ranged interactions. This is not provided by the “local” MLP framework employed here. Note that promoting MLP free energies to the *ab initio* level by FEP only incurs the cost of a few tens of *ab initio* energy and force evaluations for configurations sampled by the MLPs, and thus constitutes a reliable *and* computationally efficient means of predicting the relative stability of polymorphs.

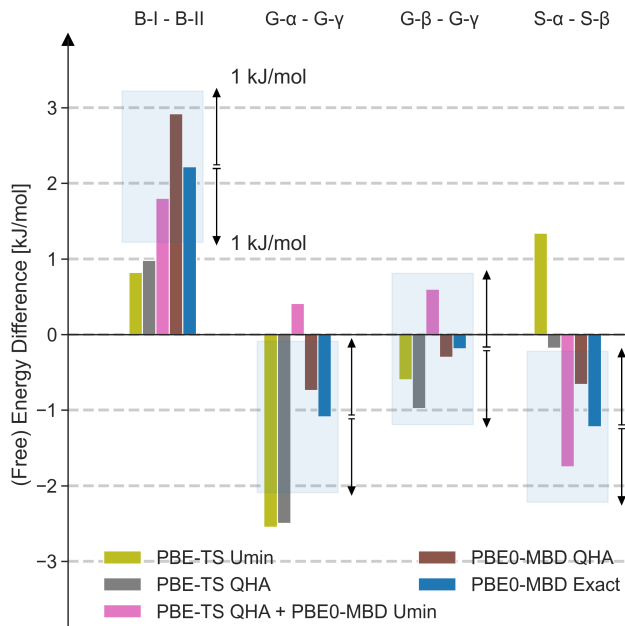


Figure 4. MLP (free) energy differences between forms I and II of benzene (B-I and B-II),  $\alpha$ ,  $\beta$ , and  $\gamma$ -glycine (G- $\alpha$ , G- $\beta$  and G- $\gamma$ ), and  $\alpha$  and  $\beta$ -succinic acid (S- $\alpha$  and S- $\beta$ ) at different tiers of accuracy: PBE-TS level static-lattice energy difference (Umin) for the optimized cells (green), bare PBE-TS based QHA (gray) and single-point PBE0-MBD corrected QHA (pink), full PBE0-MBD based QHA (brown), and the exact PI free energy difference (blue). The shaded region indicates free energy differences within 1 kJ/mol of the respective exact PI result as a guide to the eye.

In order to highlight the advantages of choosing the approach proposed here over established and streamlined approximate methods for ranking stabilities in CSP, we assess the limitations of the most widely used approximate methods, prefaced by acknowledging their successes for a wide range of applications [39, 43, 45]. To this end we restrict ourselves to MLP free energies and compare the respective approximate (free) energy differences between polymorphs to the corresponding exact MLP Gibbs free energies. The most widespread approach is to use lattice energies of variable-cell geometry-optimized structures as a proxy for free energies [38]. These are typically calculated using semi-local DFT, for instance with the PBE functional and a TS dispersion-correction (PBE-TS) [62–64]. Fig. 4 shows that this incurs errors in free energy differences up to above 2 kJ/mol. A second, more accurate approach is to estimate finite-temperature free energies within the quasi-harmonic approximation (QHA) [65]. For our systems this reduces the typical errors to just above 1 kJ/mol (see Fig. 4). The arguably most reli-

able strategy employed to date [43] is to correct QHA free energies obtained using semi-local DFT based on a single, hybrid-functional DFT calculation [39, 43]. For our systems this correction only leads to a small improvement, with the typical error not dipping significantly below 1 kJ/mol. Unfortunately, none of these approaches reproduce the correct stability order for all systems. Given that errors of 1 kJ/mol are often considered to be within “chemical accuracy”, it is worth emphasising that the compounds considered here are not hand-picked, “pathological” examples, but expected to be representative of many (bio-)molecular compounds.

Notably, performing the full QHA at the hybrid-functional level (to account for the interplay of Pauli repulsion and many-body electronic dispersion with nuclear quantum effects and thermal expansion within a harmonic approximation) halves the average error in free energy differences, and seemingly makes the QHA competitive with the rigorous PI approach. It is therefore worthwhile to put the respective costs of the calculations into perspective. For glycine, as the most costly example, the 4,000 unit-cell PBE0-MBD calculations constituting the reference data for the MLP add to the MLP-based PI thermodynamic integration, and the 50 supercell PBE0-MBD calculations required for the FEP to result in a total cost of around 148,000 core-hours per polymorph. For comparison, a naive harmonic approximation using finite differences at the same level of theory and for the same simulation supercell would require 1,440 supercell PBE0-MBD calculations costing around 1.7 million core-hours per polymorph (which can be reduced by around a factor of four by using non-diagonal supercells to probe individual  $k$ -points [66]). Despite a focus on universal applicability over efficiency, the cost the above rigorous Gibbs free energies is thus small compared to the estimated cost of calculating PBE0-MBD free energies even within the harmonic approximation.

Although polymorph stability at ambient conditions is of particular significance, the phase behaviour at general thermodynamic conditions is of great interest for controlling polymorph crystallization. Temperature arguably constitutes the most easily tuneable thermodynamic constraint and is often key to crystallizing different polymorphs from the melt [15]. While we reserve evaluations of the full temperature phase-diagrams for future work, gradients of Gibbs free energies, including the molar volume, entropy, and constant-pressure heat capacity, come as a compliment of the above calculations and provide indication regarding prospective changes in relative stability and thus the monotropic or enantiotropic nature of polymorphs. Indeed these quantities are directly related to several “thermodynamic rules of thumb” for determining stability trends from experimental densities, melting temperatures, and heats

of transformation and fusion [15]. For instance, approximating Gibbs free energy differences to depend linearly on pressure,  $\Delta G(p, T) \approx \Delta G(p_0, T) + (p - p_0)\Delta V$ , we can estimate form II of benzene to become thermodynamically over the ambient pressure form I at 1.4 GPa (at 100 K), which is in good agreement with the experimentally determined transition pressure of 1.5 GPa [61]. Similarly, we determine the entropies of  $\gamma$ -glycine and  $\alpha$ -succinic acid to be smaller than those of  $\alpha$ -glycine and  $\beta$ -succinic acid, respectively, making the latter the preferred high-temperature polymorphs in agreement with the experimentally observed transitions to  $\alpha$ -glycine and  $\beta$ -succinic acid at 443 K [67] and 410 K [62], respectively.

## DISCUSSION

Marrying state-of-the-art electronic structure, free energy, and machine-learning methods in a widely applicable framework renders rigorous, predictive free energy calculations not just computationally viable, but efficient. On top of highly accurate Gibbs free energies at the chosen temperatures and pressures, our simulations provide (for free) entropies and molar volumes, which constitute valuable indicators of prospective phase-transitions, in direct analogy with the “thermodynamic rules of thumbs” used by experimentalists to assess the monotropic or enantiotropic nature of polymorphs. Further, a rigorous assessment of thermally-induced phase-transitions can be obtained at the cost of an additional temperature thermodynamic integration for each polymorph. Indeed, our framework naturally generalizes to the calculation of full  $p - T$  phase diagrams.

Notably, the resultant predictions of thermodynamic stability are very robust with respect to the nature of the candidate polymorphs, since dynamic disorder, thermal expansion, conformational relaxation of the molecular units within the crystal structure, and potential (dynamic) instabilities of candidate polymorphs are automatically accounted for. For instance, our calculations account for the suppressed rotation of the amine groups in glycine [68] as well as the dynamic disorder of the protons in succinic acid. Furthermore, the dynamical nature of our simulations collapses redundant sets of minimum potential energy structures, as are common in CSP, onto the typically much smaller number of associated free energy minima [69] (prior to full free energy computation), thereby eliminating a common headache in traditional CSP studies. Finally, calculating Gibbs free energies at experimental conditions allows direct comparison with experimental data, eliminating the need to extrapolate experimental data to 0 K and subtracting zero-point effects in an *ad-hoc* fashion, which is prone to errors.

Despite the demonstrated power of the described

scheme for free energy calculations, some limitations to its universality must be acknowledged, starting with the empiricism involved in selecting the exchange-correlation functional and dispersion correction used in the DFT calculations. Indeed, truly resolving the greater stability of  $\gamma$ -glycine compared to  $\alpha$ -glycine may require a more accurate description of electronic structure. The framework extends naturally to predictions of Gibbs free energies based on quantum-chemical electronic structure methods such as MP2 [70], RPA [71], coupled cluster [72] or quantum Monte Carlo [73], some of which are systematically improvable, and can thereby be rendered truly *ab initio*. While these come at an increased computational cost per calculation,  $\Delta$ -learning schemes [74] combined with active learning strategies [75], promise to minimize the number of quantum-chemical calculations required to train accurate MLPs and thus to keep the overall costs in check. Meanwhile, uncertainty estimation for MLP predictions [76] may facilitate determining if a FEP correction is required. Recent investigations of the incompleteness of representations of atomic structures [57], the use of higher body-order corrections [77], and means of including long-ranged interactions [56] pave the way for MLPs capable of reproducing quantum-chemical energies with sub-kJ/mol accuracy, promising to eliminate the need for FEP to the reference level of theory.

Indeed, the observation that MLP-based free energies already reproduce the reference free energy differences to within around 1 kJ/mol suggests that MLPs are already suitable for screening CSP data at the level of configurational energies, as recently demonstrated in Ref. [78], as well as more accurate free energies, prior to predictive *ab initio* free energy calculations for the most promising candidates. We thus envisage the use of MLP-based free energy calculations to become common practice in CSP applications.

The demonstrated framework promises to recover accurate stability rankings of more flexible and more challenging systems such as salts, hydrates and co-crystals of pharmaceutical importance, and functional materials such as metal organic frameworks, and porous organic crystals. More insights on how a particular molecular crystal can be synthesized, or quantification of decay rates into more stable structures can be obtained by studying kinetic stability. The demonstrated accuracy of MLP-based free energy calculations sets the stage for future studies of kinetic effects as well as full  $p$ - $T$  phase-diagrams using MLPs in a reliable and computationally efficient manner.

## ACKNOWLEDGEMENTS

VK acknowledges funding from the Swiss National Science Foundation (SNSF), Project P2ELP2\_191678,

and support from the NCCR MARVEL, funded by the SNSF. EAE acknowledges funding from Trinity College, Cambridge. The authors thank Benjamin Shi, Daan Frenkel, Angelos Michaelides, Sally Price and Michele Ceriotti for valuable suggestions on the manuscript. EAE and VK acknowledges allocation of CPU hours by CSCS under Project IDs s960 and s1000.

## METHODS

**Machine-learning potentials:** We have constructed Behler-Parinello type neural network potentials [79] for benzene, glycine, and succinic acid using the n2p2 code [80]. In this framework, structures are encoded in terms of local atom-centered symmetry functions (SF) [79]. Initial sets of SFs were generated following the recipe of Ref. [81]. Based on the same reference structure-property data subsequently used for training, the 128 (benzene and succinic acid) and 256 (glycine) most informative SFs were extracted via PCovCUR selection [82].

Our data is based on Langevin-thermostatted PI NVT simulations at 300 K, performed using the i-Pi force engine [83] coupled to DFTB+ [84] calculations with the 3ob parametrization [85]. For each polymorph multiple cells were simulated, rescaling the experimental cell lengths and angles by up to 10% and 5%, respectively. All trajectories for a given compound were concatenated and farthest-point sampled [86–88] to extract the most distinct configurations for feature selection and MLP training. Subsequently, *ab initio* reference energies and forces were evaluated for said configurations.

To minimise the computational cost of the reference calculations the MLPs are composed of a baseline potential trained to reproduce energies and forces from more affordable PBE-DFT [89] calculations with a TS dispersion correction [90] (PBE-TS), and a  $\Delta$ -learning [74] correction trained (on ten times fewer training data) to reproduce the difference between the baseline and more expensive calculations with the hybrid PBE0 functional [91, 92] and the MBD dispersion correction [93, 94] (PBE0-MBD). For a separate test set, the MLPs reproduce PBE0-MBD energies with root-mean-square errors of 1.2 kJ/mol for benzene, 1.6 kJ/mol for glycine, and 2.3 kJ/mol for succinic acid, respectively.

**Ab initio DFT calculations:** BE0+MBD calculations were performed using FHI-aims [95–97] with the standard FHI-aims “intermediate” basis sets and a Monkhorst-Pack k-point grid [98] with a maximum spacing of  $0.06 \times 2\pi \text{ \AA}^{-1}$ . The PBE-TS baseline calculations for a  $\Delta$ -learning approach were performed using Quantum Espresso v6.3, the same k-point grid, a wavefunction cut-off energy of 100 Rydberg, and the optimised, norm-conserving Vanderbilt pseudopotentials from Ref. [99].

**Free energy methods:** For each polymorph the average cell was determined using MLP based path integral (PI) NST simulations [100] at the desired inverse temperature  $\beta$ , accounting for anharmonic quantum nuclear motion and anisotropic cell fluctuations. The difference between the Gibbs and Helmholtz free energies is computed from a MLP based PI NPT simulation based on its average cell is

$$G_{\text{MLP}}(P^{\text{ext}}, \beta) - A_{\text{MLP}}(V, \beta) = P^{\text{ext}}V + \beta^{-1} \ln \rho(V|P^{\text{ext}}, \beta),$$

where  $\rho(V|P^{\text{ext}}, \beta)$  is the probability of observing the cell volume  $V$  at external pressure  $P^{\text{ext}}$  and inverse temperature  $\beta$ . A standard Kirkwood construction [101] that transforms the

Hamiltonian from a harmonic to an anharmonic one provides the difference between the anharmonic and the harmonic quantum Helmholtz free energies:

$$A_{\text{MLP}}(V, \beta) - A_{\text{MLP}}^{\text{har}}(V, \beta) = \int_0^1 d\lambda \left\langle \hat{H}_{\text{MLP}} - \hat{H}_{\text{MLP}}^{\text{har}} \right\rangle_{V, \beta, \hat{H}_\lambda},$$

where  $\hat{H}_\lambda$  is the Hamiltonian of the MLP alchemical system with the potential  $U_\lambda \equiv \lambda U_{\text{MLP}} + (1 - \lambda)U_{\text{MLP}}^{\text{har}}$ , and  $\langle \cdot \rangle$  is the ensemble average computed from a PI NVT simulation. The reference absolute harmonic Helmholtz free energy is obtained from a harmonic approximation using

$$A_{\text{MLP}}^{\text{har}}(V, \beta) = U_{\text{MLP}}(V) + \sum_i \left[ \frac{1}{2} \hbar \omega_i + \beta^{-1} \ln \left( 1 - e^{-\beta \hbar \omega_i} \right) \right],$$

where  $\omega_i$  is the frequency of the  $i$ -th phonon mode. In a final step, the *ab initio* Gibbs free energy is obtained from its MLP counterpart by free energy perturbation using

$$G(P^{\text{ext}}, \beta) - G_{\text{MLP}}(P^{\text{ext}}, \beta) = -\beta^{-1} \ln \left\langle e^{-\beta(U - U_{\text{MLP}})} \right\rangle_{P^{\text{ext}}, \beta, \hat{H}_{\text{MLP}}}.$$

- 
- [1] S. Datta and D. J. W. Grant, *Nature Reviews Drug Discovery* **3**, 42 (2004).
- [2] S. R. Forrest, *Nature* **428**, 911 (2004).
- [3] T. Tozawa, J. T. A. Jones, S. I. Swamy, S. Jiang, D. J. Adams, S. Shakespeare, R. Clowes, D. Bradshaw, T. Hasell, S. Y. Chong, C. Tang, S. Thompson, J. Parker, A. Trewin, J. Bacsá, A. M. Z. Slawin, A. Steiner, and A. I. Cooper, *Nature Materials* **8**, 973 (2009).
- [4] H. Hondoh and S. Ueno, *Progress in Crystal Growth and Characterization of Materials Special Issue: Recent Progress on Fundamentals and Applications of Crystal Growth; Proceedings of the 16th International Summer School on Crystal Growth (ISSCG-16)*, **62**, 398 (2016).
- [5] J. Yang, C. T. Hu, X. Zhu, Q. Zhu, M. D. Ward, and B. Kahr, *Angewandte Chemie* **129**, 10299 (2017).
- [6] K. Honer, E. Kalfaoglu, C. Pico, J. McCann, and J. Baltrusaitis, *ACS Sustainable Chemistry & Engineering* **5**, 8546 (2017).
- [7] D. Gentili, M. Gazzano, M. Melucci, D. Jones, and M. Cavallini, *Chemical Society Reviews* **48**, 2502 (2019).
- [8] D. Chistyakov and G. Sergeev, *Pharmaceutics* **12** (2020), 10.3390/pharmaceutics12010034.
- [9] A. J. Cruz-Cabeza, S. M. Reutzel-Edens, and J. Bernstein, *Chemical Society Reviews* **44**, 8619 (2015).
- [10] S. R. Chemburkar, J. Bauer, K. Deming, H. Spiwek, K. Patel, J. Morris, R. Henry, S. Spanton, W. Dziki, W. Porter, J. Quick, P. Bauer, J. Donaubauer, B. A. Narayanan, M. Soldani, D. Riley, and K. McFarland, *Organic Process Research & Development* **4**, 413 (2000).
- [11] K. R. Chaudhuri, *Expert Opinion on Drug Delivery* **5**, 1169 (2008).
- [12] I. B. Rietveld and R. Céolin, *Journal of Pharmaceutical Sciences* **104**, 4117 (2015).
- [13] D.-K. Bučar, R. W. Lancaster, and J. Bernstein, *Angewandte Chemie International Edition* **54**, 6972 (2015).
- [14] S. L. Morissette, O. Almarsson, M. L. Peterson, J. F. Remenar, M. J. Read, A. V. Lemmo, S. Ellis, M. J. Cima, and C. R. Gardner, *Advanced Drug Delivery Reviews* **56**, 275 (2004).
- [15] E. H. Lee, *Asian Journal of Pharmaceutical Sciences* **9**, 163 (2014).
- [16] S. L. Price, *Chemical Society Reviews* **43**, 2098 (2014).
- [17] J. Nyman and S. M. Reutzel-Edens, *Faraday Discussions* **211**, 459 (2018).
- [18] G. L. Perlovich, L. K. Hansen, and A. Bauer-Brandl, *Journal of Thermal Analysis and Calorimetry* **66**, 699 (2001).
- [19] V. A. Drebuschak, Y. A. Kovalevskaya, I. E. Paukov, and E. V. Boldyreva, *Journal of Thermal Analysis and Calorimetry* **74**, 109 (2003).
- [20] V. A. Drebuschak, E. V. Boldyreva, Y. A. Kovalevskaya, I. E. Paukov, and T. N. Drebuschak, *Journal of Thermal Analysis and Calorimetry* **79**, 65 (2005).
- [21] C. J. Pickard and J. Needs, *Nature Physics* **3**, 473 (2007).
- [22] B. Monserrat, R. J. Needs, E. Gregoryanz, and C. J. Pickard, *Phys. Rev. B* **94**, 134101 (2016).
- [23] Y. M. Ma, M. Eremets, A. R. Oganov, Y. Xie, I. Trojan, S. Medvedev, A. O. Lyakhov, M. Valle, and V. Prakapenka, *Nature* **458**, 182 (2009).
- [24] Y. Li, J. Hao, H. Liu, Y. Li, and Y. Ma, *J. Chem. Phys.* **140**, 174712 (2014).
- [25] I. Errea, M. Calandra, C. J. Pickard, J. Nelson, R. J. Needs, Y. Li, H. Liu, Y. Zhang, Y. Ma, and F. Mauri, *Phys. Rev. Lett.* **114**, 157004 (2015).
- [26] A. P. Drozdov, P. P. Kong, V. S. Minkov, S. P. Besedin, M. A. Kuzovnikov, S. Mozaffari, L. Balicas, F. F. Balakirev, D. E. Graf, V. B. Prakapenka, E. Greenberg, D. A. Knyazev, M. Tkacz, and M. I. Eremets, *Nature* **569**, 528 (2019).
- [27] H. L. Zhuang and R. G. Hennig, *Journal of the Minerals, Metals & Materials Society* **66**, 366 (2014).
- [28] N. Mounet, M. Gibertini, P. Schwaller, D. Campi, A. Merkys, A. Marrazzo, T. Sohier, I. Eligio Castelli, A. Cepellotti, G. Pizzi, and N. Marzari, *Nature Nanotechnology* **13**, 246 (2018).
- [29] A. Marrazzo, M. Gibertini, D. Campi, N. Mounet, and N. Marzari, *Phys. Rev. Lett.* **120**, 117701 (2018).
- [30] P. E. A. Turchi, P. Söderlind, and A. I. Landa, *Journal of the Minerals, Metals & Materials Society* **66**, 375 (2014).
- [31] B. D. Conduit, N. G. Jones, H. J. Stone, and G. J. Conduit, *Materials & Design* **131**, 358 (2017).

- [32] P. Sarker, T. Harrington, C. Toher, C. Oses, M. Samiee, J.-P. Maria, D. W. Brenner, K. S. Vecchio, and S. Curtarolo, *Nature Communications* **9**, 4980 (2018).
- [33] J. P. M. Lommerse, W. D. S. Motherwell, H. L. Ammon, J. D. Dunitz, A. Gavezzotti, D. W. M. Hofmann, F. J. J. Leusen, W. T. M. Mooij, S. L. Price, B. Schweizer, M. U. Schmidt, B. P. v. Eijck, P. Verwer, and D. E. Williams, *Acta Crystallographica Section B: Structural Science* **56**, 697 (2000).
- [34] W. D. S. Motherwell, H. L. Ammon, J. D. Dunitz, A. Dzyabchenko, P. Erk, A. Gavezzotti, D. W. M. Hofmann, F. J. J. Leusen, J. P. M. Lommerse, W. T. M. Mooij, S. L. Price, H. Scheraga, B. Schweizer, M. U. Schmidt, B. P. v. Eijck, P. Verwer, and D. E. Williams, *Acta Crystallographica Section B: Structural Science* **58**, 647 (2002).
- [35] G. M. Day, W. D. S. Motherwell, H. L. Ammon, S. X. M. Boerrigter, R. G. Della Valle, E. Venuti, A. Dzyabchenko, J. D. Dunitz, B. Schweizer, B. P. van Eijck, P. Erk, J. C. Facelli, V. E. Bazterra, M. B. Ferraro, D. W. M. Hofmann, F. J. J. Leusen, C. Liang, C. C. Pantelides, P. G. Karamertzanis, S. L. Price, T. C. Lewis, H. Nowell, A. Torrissi, H. A. Scheraga, Y. A. Arnautova, M. U. Schmidt, and P. Verwer, *Acta Crystallographica Section B: Structural Science* **61**, 511 (2005).
- [36] G. M. Day, T. G. Cooper, A. J. Cruz-Cabeza, K. E. Hejczyk, H. L. Ammon, S. X. M. Boerrigter, J. S. Tan, R. G. Della Valle, E. Venuti, J. Jose, S. R. Gadre, G. R. Desiraju, T. S. Thakur, B. P. van Eijck, J. C. Facelli, V. E. Bazterra, M. B. Ferraro, D. W. M. Hofmann, M. A. Neumann, F. J. J. Leusen, J. Kendrick, S. L. Price, A. J. Misquitta, P. G. Karamertzanis, G. W. A. Welch, H. A. Scheraga, Y. A. Arnautova, M. U. Schmidt, J. van de Streek, A. K. Wolf, and B. Schweizer, *Acta Crystallographica Section B: Structural Science* **65**, 107 (2009).
- [37] D. A. Bardwell, C. S. Adjiman, Y. A. Arnautova, E. Bartashevich, S. X. M. Boerrigter, D. E. Braun, A. J. Cruz-Cabeza, G. M. Day, R. G. Della Valle, G. R. Desiraju, B. P. van Eijck, J. C. Facelli, M. B. Ferraro, D. Grillo, M. Habgood, D. W. M. Hofmann, F. Hofmann, K. V. J. Jose, P. G. Karamertzanis, A. V. Kazantsev, J. Kendrick, L. N. Kuleshova, F. J. J. Leusen, A. V. Maleev, A. J. Misquitta, S. Mohamed, R. J. Needs, M. A. Neumann, D. Nikylov, A. M. Orendt, R. Pal, C. C. Pantelides, C. J. Pickard, L. S. Price, S. L. Price, H. A. Scheraga, J. van de Streek, T. S. Thakur, S. Tiwari, E. Venuti, and I. K. Zhitkov, *Acta Crystallographica Section B: Structural Science* **67**, 535 (2011).
- [38] A. M. Reilly, R. I. Cooper, C. S. Adjiman, S. Bhattacharya, A. D. Boese, J. G. Brandenburg, P. J. Bygrave, R. Bylisma, J. E. Campbell, R. Car, D. H. Case, R. Chadha, J. C. Cole, K. Cosburn, H. M. Cuppen, F. Curtis, G. M. Day, R. A. DiStasio Jr, A. Dzyabchenko, B. P. van Eijck, D. M. Elking, J. A. van den Ende, J. C. Facelli, M. B. Ferraro, L. Fustimolnar, C.-A. Gatsiou, T. S. Gee, R. de Gelder, L. M. Ghiringhelli, H. Goto, S. Grimme, R. Guo, D. W. M. Hofmann, J. Hoja, R. K. Hylton, L. Iuzolino, W. Jankiewicz, D. T. de Jong, J. Kendrick, N. J. J. de Klerk, H.-Y. Ko, L. N. Kuleshova, X. Li, S. Lohani, F. J. J. Leusen, A. M. Lund, J. Lv, Y. Ma, N. Marom, A. E. Masunov, P. McCabe, D. P. McMahon, H. Meekes, M. P. Metz, A. J. Misquitta, S. Mohamed, B. Monserrat, R. J. Needs, M. A. Neumann, J. Nyman, S. Obata, H. Oberhofer, A. R. Oganov, A. M. Orendt, G. I. Pagola, C. C. Pantelides, C. J. Pickard, R. Podeszwa, L. S. Price, S. L. Price, A. Pulido, M. G. Read, K. Reuter, E. Schneider, C. Schober, G. P. Shields, P. Singh, I. J. Sugden, K. Szalewicz, C. R. Taylor, A. Tkatchenko, M. E. Tuckerman, F. Vacarro, M. Vasileiadis, A. Vazquez-Mayagoitia, L. Vogt, Y. Wang, R. E. Watson, G. A. de Wijs, J. Yang, Q. Zhu, and C. R. Groom, *Acta Crystallographica Section B: Structural Science, Crystal Engineering and Materials* **72**, 439 (2016).
- [39] N. Marom, R. A. DiStasio, V. Atalla, S. Levchenko, A. M. Reilly, J. R. Chelikowsky, L. Leiserowitz, and A. Tkatchenko, *Angewandte Chemie International Edition* **52**, 6629 (2013).
- [40] M. Rossi, P. Gasparotto, and M. Ceriotti, *Physical Review Letters* **117**, 115702 (2016).
- [41] E. Schneider, L. Vogt, and M. E. Tuckerman, *Acta Crystallographica Section B: Structural Science, Crystal Engineering and Materials* **72**, 542 (2016).
- [42] H.-Y. Ko, R. A. DiStasio, B. Santra, and R. Car, *Physical Review Materials* **2**, 055603 (2018).
- [43] J. Hoja, H.-Y. Ko, M. A. Neumann, R. Car, R. A. DiStasio, and A. Tkatchenko, *Science Advances* **5**, eaau3338 (2019).
- [44] B. P. van Eijck, W. T. M. Mooij, and J. Kroon, *The Journal of Physical Chemistry B* **105**, 10573 (2001).
- [45] A. M. Reilly and A. Tkatchenko, *Physical Review Letters* **113**, 055701 (2014).
- [46] J. Nyman and G. M. Day, *CrystEngComm* **17**, 5154 (2015).
- [47] D. Marx and M. Parrinello, *The Journal of Chemical Physics* **104**, 4077 (1996).
- [48] V. Kapil, E. Engel, M. Rossi, and M. Ceriotti, *Journal of Chemical Theory and Computation* **15**, 5845 (2019).
- [49] B. Cheng, E. A. Engel, J. Behler, C. Dellago, and M. Ceriotti, *Proceedings of the National Academy of Sciences* **116**, 1110 (2019).
- [50] Y. Zuo, C. Chen, X. Li, Z. Deng, Y. Chen, J. Behler, G. Csányi, A. V. Shapeev, A. P. Thompson, M. A. Wood, and S. P. Ong, *The Journal of Physical Chemistry A* **124**, 731 (2020).
- [51] A. M. Reilly and A. Tkatchenko, *J. Chem. Phys.* **139**, 024705 (2013).
- [52] G. J. O. Beran, *Chem. Rev.* **116**, 5567 (2016).
- [53] B. Monserrat, J. G. Brandenburg, E. A. Engel, and B. Cheng, *Nature Communications* **11**, 5757 (2020).
- [54] T. Morawietz, A. Singraber, C. Dellago, and J. Behler, *Proceedings of the National Academy of Sciences* **113**, 8368 (2016).
- [55] R. Jinnouchi, F. Karsai, and G. Kresse, *Physical Review B* **100**, 014105 (2019).
- [56] A. Grisafi and M. Ceriotti, *The Journal of Chemical Physics* **151**, 204105 (2019).



- [57] S. N. Pozdnyakov, M. J. Willatt, A. P. Bartók, C. Ortner, G. Csányi, and M. Ceriotti, *Physical Review Letters* **125**, 166001 (2020).
- [58] A. Katrusiak, M. Podsiadło, and A. Budzianowski, *Crystal Growth & Design* **10**, 3461 (2010).
- [59] A. Dawson, D. R. Allan, S. A. Belmonte, S. J. Clark, W. I. F. David, P. A. McGregor, S. Parsons, C. R. Pulham, and L. Sawyer, *Crystal Growth & Design* **5**, 1415 (2005).
- [60] J.-L. Leviel, G. Auvert, and J.-M. Savariault, *Acta Crystallographica Section B: Structural Crystallography and Crystal Chemistry* **37**, 2185 (1981).
- [61] K. H. Yurtseven and M. Senol, *Acta Physica Polonica A* **124**, 698 (2013).
- [62] P. Lucaioli, E. Nauha, I. Gimondi, L. S. Price, R. Guo, L. Iuzzolino, I. Singh, M. Salvalaglio, S. L. Price, and N. Blagden, *CrystEngComm* **20**, 3971 (2018).
- [63] J. G. Brandenburg and S. Grimme, *Acta Crystallographica Section B: Structural Science, Crystal Engineering and Materials* **72**, 502 (2016).
- [64] J. v. d. Streek and M. A. Neumann, *CrystEngComm* **13**, 7135 (2011).
- [65] J. Hoja, A. M. Reilly, and A. Tkatchenko, *WIREs Computational Molecular Science* **7**, e1294 (2017).
- [66] J. H. Lloyd-Williams and B. Monserrat, *Phys. Rev. B* **92**, 184301 (2015).
- [67] A. Dawson, D. R. Allan, S. A. Belmonte, S. J. Clark, W. I. F. David, P. A. McGregor, S. Parsons, C. R. Pulham, and L. Sawyer, *Crystal Growth and Design* **5**, 1415 (2005).
- [68] K. Yamauchi, Shigeki, and K. I. Ando, *Journal of Molecular Structure* **602-603**, 9 (2002).
- [69] N. F. Francia, L. S. Price, J. Nyman, S. L. Price, and M. Salvalaglio, *Crystal Growth & Design* **20**, 6847 (2020).
- [70] C. Červinka and G. J. O. Beran, *Chemical Science* **9**, 4622 (2018).
- [71] J. Klimeš, *The Journal of Chemical Physics* **145**, 094506 (2016).
- [72] T. Gruber, K. Liao, T. Tsatsoulis, F. Hummel, and A. Grüneis, *Physical Review X* **8**, 021043 (2018).
- [73] A. Zen, J. G. Brandenburg, J. Klimeš, A. Tkatchenko, D. Alfè, and A. Michaelides, *Proceedings of the National Academy of Sciences* **115**, 1724 (2018).
- [74] R. Ramakrishnan, P. O. Dral, M. Rupp, and O. A. von Lilienfeld, *Journal of Chemical Theory and Computation* **11**, 2087 (2015).
- [75] C. Schran, K. Brezina, and O. Marsalek, *The Journal of Chemical Physics* **153**, 104105 (2020).
- [76] F. Musil, M. J. Willatt, M. A. Langovoy, and M. Ceriotti, *J. Chem. Theory Comput.* **15**, 906 (2019).
- [77] J. Nigam, S. Pozdnyakov, and M. Ceriotti, *The Journal of Chemical Physics* **153**, 121101 (2020).
- [78] S. Wengert, G. Csányi, K. Reuter, and J. T. Margraf, *Chemical Science* (2021), 10.1039/D0SC05765G.
- [79] J. Behler and M. Parrinello, *Phys. Rev. Lett.* **98**, 146401 (2007).
- [80] A. Singraber, J. Behler, and C. Dellago, *Journal of Chemical Theory and Computation* **15**, 1827 (2019).
- [81] G. Imbalzano, A. Anelli, D. Giofrè, S. Klees, J. Behler, and M. Ceriotti, *Journal of Chemical Physics* **148**, 241730 (2018).
- [82] R. K. Cersonsky, B. A. Helfrecht, E. A. Engel, and M. Ceriotti, (2021), arXiv:2012.12253.
- [83] V. Kapil, M. Rossi, O. Marsalek, R. Petraglia, Y. Litman, T. Spura, B. Cheng, A. Cuzzocrea, R. H. Meißner, D. M. Wilkins, B. A. Helfrecht, P. Juda, S. P. Bienvenue, W. Fang, J. Kessler, I. Poltavsky, S. Vandenbrande, J. Wieme, and M. Ceriotti, *Computer Physics Communications* **236**, 214 (2018).
- [84] “DFTB+, a software package for efficient approximate density functional theory based atomistic simulations: The Journal of Chemical Physics: Vol 152, No 12,” .
- [85] T. Krüger, M. Elstner, P. Schiffels, and T. Frauenheim, *The Journal of Chemical Physics* **122**, 114110 (2005).
- [86] Y. Eldar, M. Lindenbaum, M. Porat, and Y. Y. Zeevi, *IEEE Transactions on Image Processing* **6**, 1305 (1997).
- [87] M. Ceriotti, G. A. Tribello, and M. Parrinello, *Journal of Chemical Theory and Computation* **9**, 1521 (2013).
- [88] R. J. G. B. Campello, D. Moulavi, A. Zimek, and J. Sander, *ACM Trans. Knowl. Discov. Data* **10**, 5 (2015).
- [89] J. P. Perdew, K. Burke, and M. Ernzerhof, *Physical Review Letters* **77**, 3865 (1996).
- [90] A. Tkatchenko and M. Scheffler, *Physical Review Letters* **102**, 073005 (2009).
- [91] J. P. Perdew, M. Ernzerhof, and K. Burke, *Journal of Chemical Physics* **105**, 9982 (1996).
- [92] C. Adamo and V. Barone, *Journal of Chemical Physics* **110**, 6158 (1999).
- [93] A. Tkatchenko, R. A. Di Stasio Jr, R. Car, and M. Scheffler, *Physical Review Letters* **108**, 236402 (2012).
- [94] A. Ambrosetti, A. M. Reilly, R. A. Di Stasio Jr, and A. Tkatchenko, *Journal of Chemical Physics* **140**, 018A508 (2014).
- [95] V. Blum, R. Gehrke, F. Hanke, P. Havu, V. Havu, X. Ren, K. Reuter, and M. Scheffler, *Computer Physics Communications* **180**, 2175 (2009).
- [96] X. Ren, P. Rinke, V. Blum, J. Wierfink, A. Tkatchenko, A. Sanfilippo, K. Reuter, and M. Scheffler, *New Journal of Physics* **14**, 053020 (2012).
- [97] S. Levchenko, X. Ren, J. Wierfink, R. Johanni, P. Rinke, V. Blum, and M. Scheffler, *Computer Physics Communications* **192**, 60 (2015).
- [98] H. J. Monkhorst and J. D. Pack, *Physical Review B* **13**, 5188 (1976).
- [99] M. Schlipf and F. Gygi, *Computer Physics Communications* **196**, 36 (2015).
- [100] P. Raiteri, J. D. Gale, and G. Bussi, *Journal of Physics: Condensed Matter* **23**, 334213 (2011).
- [101] D. Frenkel and A. J. C. Ladd, *The Journal of Chemical Physics* **81**, 3188 (1984).